Solid State Sciences 11 (2009) 1625–1630

Contents lists available at ScienceDirect

Solid State Sciences

journal homepage: www.elsevier.com/locate/ssscie

Fabrication and characterization of three-dimensionally ordered macroporous niobium oxide

Li Yao [a], Xin Wuhong [a], Zhao Jiupeng [b,*], Meng Xiangdong [a]

[a] Center for Composite Materials, Harbin Institute of Technology, No. 92 Xida zhi Street, Harbin 150001, PR China
[b] School of Chemical Engineering and Technology, Harbin Institute of Technology, No. 92 Xida zhi Street, Harbin 150001, PR China

ARTICLE INFO

Article history:
Received 1 April 2009
Received in revised form 5 June 2009
Accepted 7 June 2009
Available online 16 June 2009

Keywords:
3-DOM niobium oxide
Aqueous organic gel process
Colloidal crystal
Polystyrene (PS) template

ABSTRACT

Three-dimensionally ordered macroporous (3-DOM) niobium oxide was fabricated by aqueous organic gel method through the interstitial spaces between polystyrene spheres assembled on glass substrates. Freshly precipitated hydrous niobium oxide ($Nb_2O_5 \cdot nH_2O$), which was prepared starting from Nb_2O_5, was used in combination with citric acid in an aqueous solution and then was transferred as a niobium source to synthesize 3-DOM Nb_2O_5. The morphologies of porous Nb_2O_5 were characterized by scanning electron microscope (SEM). The thermal decomposition and phase composition of 3-DOM Nb_2O_5 were investigated by Fourier transform infrared spectroscopy (FT-IR), Thermogravimetric–differential thermal analysis (TG–DTA), X-ray diffraction (XRD) and X-ray photoelectron spectroscopy (XPS).

1. Introduction

Three-dimensionally ordered macroporous (3-DOM) materials with controllable pore size and highly ordered structures have received considerable interests for their potential applications [1,2]. The unique ability of controlling the propagation of light makes 3-DOM structure ideal materials for optical devices. Due to their large inner surface and connective air spheres, these materials can be used as catalytic supporters or chemical filters. In addition, the 3-DOM materials have been exploited in many applications in other areas, such as sensors, thermal and acoustic insulators [3,4]. The fabrication of highly ordered niobium oxide will also bear high application potential as gas sensors, catalysts, and optical devices, which could strongly benefit from the corresponding increase in surface area. Previous researchers have also paid attention to the fabrication of ordered Nb_2O_5 [5,6]. Choi et al. have prepared nanoporous Nb_2O_5 films through making a protective layer in outermost oxide based on anodization–annealing–anodization, but the order parameter and aspect ratio of the products are not very appealing [7]. Ying et al. have reported the synthesis of mesoporous Nb_2O_5 with the same low aspect ratio compared to the macroporous products [8,9]. Orilall et al. have successfully fabricated Nb_2O_5 in 3-DOM structure, whereas the article aims mainly at introducing a novel kind of templates [10]. Research focuses on the fabrication and characterization of Nb_2O_5 in this structure has not been reported.

3-DOM materials can be fabricated in three stages: first, monodisperse polystyrene (PS) spheres thin films are formed on glass substrates by capillary force during the evaporation of the dispersion medium to prepare colloidal templates; second, interstices between PS spheres are infiltrated with desired materials; third, removal of the colloidal templates by calcination or chemical etching to obtain three-dimensionally ordered macroporous frameworks. Several methods have been applied to introduce the desired materials inside the templates such as chemical vapor deposition, nano-particle infiltration, electrodeposition, chemical precipitation and sol–gel process [11–13]. Sol–gel process based upon hydrolysis–condensation of alkoxides has been successfully applied to the synthesis of 3-DOM materials. Alkoxides of niobium are most frequently used as starting materials in the sol–gel synthesis of Nb-based complex oxides, but the niobium alkoxides are expensive, extremely sensitive to moisture and have to be processed under a strictly dry atmosphere, which hinder the research progress in the fabrication of these important materials with 3-DOM structure. Orilall et al. adopted ammonium hexafluoroniobate [NH_4NbF_6] and boric acid as starting materials, the filling materials were formed in the chemical reaction which made the infiltration uncontrollable [10]. For these reasons, we propose for the first time the synthesis of 3-DOM Nb_2O_5 by using aqueous organic gel method, the filling materials of which are

* Corresponding author.
E-mail address: jpzhaohit@gmail.com (J.P. Zhao).

1293-2558/$ – see front matter
doi:10.1016/j.solidstatesciences.2009.06.005

prepared before the infiltration process. This method is based on chelating or complexing between metal cations and polyfunctional carboxylic acid, and has been intensively used for the preparation of polycation oxide ceramic powders or thin films [14–16]. The chelation process occurs during the mixing of cations and polyfunctional carboxylic acid in an aqueous solution to form soluble metal carboxylate complexes which can form the desired compound after firing at elevated temperatures. This method has the advantages of using common reagents, low cost, homogeneous mixing at molecule-level, good stoichiometric control, low processing temperature, use of an aqueous based processing system and no need for a special atmosphere. Despite of these advantages, to the best of our knowledge there are no papers that describe the preparation of 3-DOM niobium oxide by using aqueous organic gel method.

In this paper, highly ordered macroporous Nb_2O_5 was prepared by aqueous organic gel method from the water-soluble Nb–citric complex with templates of PS spheres and the problem mentioned above is circumvented successfully.

2. Experimental

2.1. Materials

Reagents used were styrene (C_8H_8, 99.99%), potassium persulfate ($K_2S_2O_8$, 99%), Nb_2O_5, hydrofluoric acid, ammonium oxalate, ammonia solution, citric acid and isopropyl alcohol. Water used in all experiments was purified with a resistivity greater than 18 ΩM/cm.

2.2. Synthesis of 3-DOM Nb_2O_5

Monodisperse PS spheres with an average diameter of 368 nm were obtained by using an emulsifier-free emulsion polymerization technique [17]. Microslides (10×60 mm) were used as substrates for PS template growth. PS thin film colloidal crystals were grown by using controlled vertical drying method, which has been previously reported [18].

For the preparation of Nb–citric complex, Nb_2O_5 was dissolved in HF to form $NbOF_5^{2-}$ or NbF_7^{2-} complexes by heating for 48 h. Aqueous solution of ammonium oxalate was added to the solution. Then ammonia solution was added with continuous stirring to form a precipitation of hydrous niobium oxide ($Nb_2O_5 \cdot nH_2O$) [19]. The precipitation was aged at 80 °C for 12 h, after which it was filtered and washed with water carefully for several times to remove the fluoride free completely [20]. The hydrous niobium oxide was then dissolved in aqueous solution of citric acid by continuous stirring and heating at 60 °C to form a transparent pale yellow Nb–citric complex. The Nb content in the solution was determined by ICP analysis. The clear transparent Nb–citric precursor, which has high stability and no precipitation for several months after preparation, can be used to infiltrate into the interstices of the templates. The concentration of the precursor was varied by dilution with water and isopropyl alcohol, ranging from 0.1 mol/L to 1.0 mol/L.

The dip-drawing method was adopted to fill the precursor into the interstices between PS spheres. The PS colloidal crystals were soaked in the precursor for 1 or 2 min and subsequently hung vertically to dry for 6 h, excess precursor was removed from the impregnated templates because of the gravity. The samples were calcined in air at 600 °C for 2 h to remove the PS templates and obtain 3-DOM Nb_2O_5 thin films.

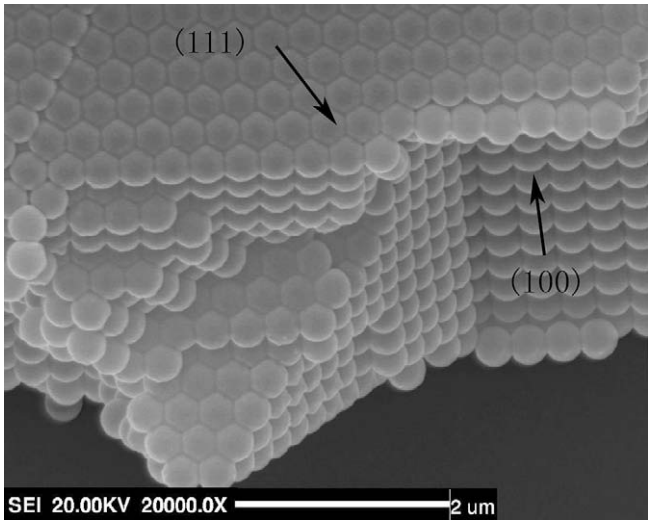

Fig. 1. SEM image showing very-ordered PS colloidal crystals template prepared by a vertical deposition.

2.3. Characterization

FT-IR spectrum was measured to study the coordinated structure of Nb–citric complex using a Perkin–Elmer Spectrum One. The sample was examined in the frequency range of 500–4,000 cm^{-1}.

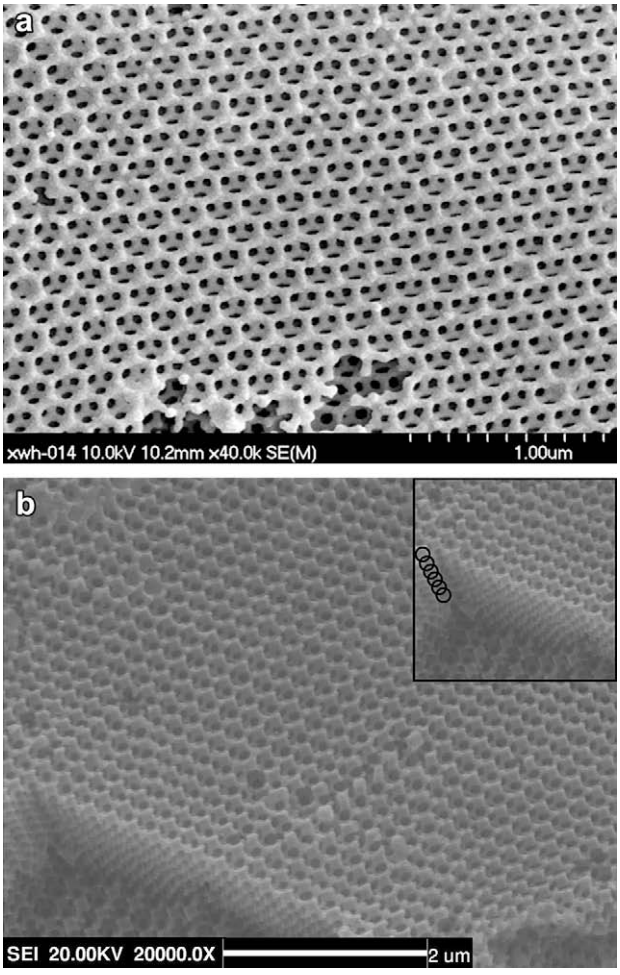

Fig. 2. SEM images showing 3-DOM Nb_2O_5 (a) top-view and (b) side-view.

A ZRY-2P TGA/DSC combined analysis equipment was used to investigate the thermal decomposition of niobium precursor. The phase composition of the 3-DOM Nb_2O_5 thin films was analyzed by using X-ray diffraction (XRD) on a Phillips X'Pert diffractometer equipped with $Cu_{K\alpha}$ radiation in the range of $2\theta = 10^\circ$–80°. The X-ray photoelectron spectroscopic (XPS) analysis of the samples was carried out on a PHI 5700 XPS system. All the binding energies were referenced to the C1s peak at 284.6 eV of surface contamination carbon. Morphological investigation was performed on a Hitachi S-4800 scanning electron microscope operated at 20 kV.

3. Results and discussion

Fig. 1 shows SEM image of PS crystal templates formed by vertical deposition from a suspension of 368 nm diameter PS spheres, which demonstrates that the monodisperse spheres are disposed in face-centered cubic lattices. The film represents a hexagonal packing array from the top-view, which indicating (111) plane of the face-centered cubic, while the side-view of the film represents a square packing array indicating (100) plane. The corresponding inverse opal structure synthesized is shown in Fig. 2. A typical top-view SEM image of an ordered macroporous Nb_2O_5 is shown in Fig. 2(a). The smooth surface of the negative replica with uniform porous size indicates that the infiltration progress is a success. A second layer of the network, with the same ordered structure, can be observed through the first layer. Fig. 2(b) shows a side-view of replica structure, which illustrates that the products were formed with a thickness more than six layers and the 3-DOM structure of the lower layer is consistent with the surface one.

The main defects in colloidal crystal templates are point defects and line defects. The prior is composed of vacancy defects and impurity defects. The vacancy defects originate from missing spheres in the templates, which have been widely reported by previous researchers [21]. The impurity defects mean that the impurities take the places of the original PS spheres. There are two kinds of impurities, one is formed by other materials, and the other is PS spheres with different diameters. In our study, the first kind of impurities can be ignored and the latter plays a key role due to the high purity of PS suspension. Fig. 3 shows SEM images of PS colloidal templates and the corresponding 3-DOM structure. As the inset image in Fig. 3(a) shown, the impurity sphere is surrounded by nine PS spheres. It can also be illustrated from the corresponding 3-DOM structure that a larger air sphere surrounded by nine smaller air spheres can be observed (Fig. 3(b), marked with a circle).

SEM images of the line defects in PS colloidal templates and the corresponding 3-DOM structure are shown in Fig. 4. Fig. 4(a) shows hexagonal packing of colloidal crystals with line defects. In Fig. 4(b), two lines of defects are formed in the 3-DOM structure

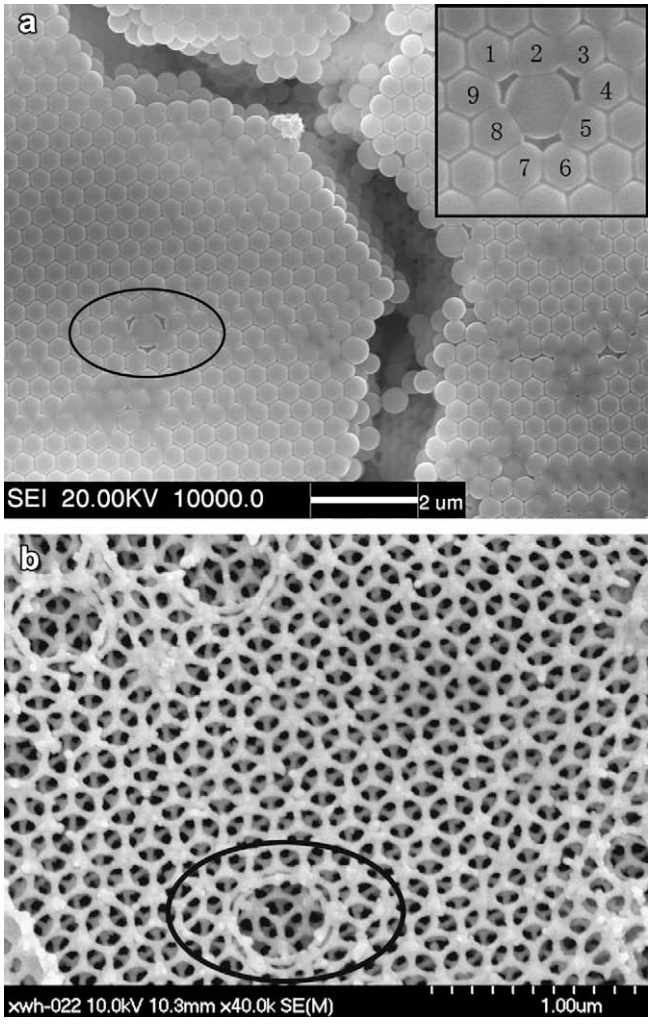

Fig. 3. SEM images showing (a) colloidal crystal with impurity defect and (b) the corresponding 3-DOM Nb_2O_5 structure.

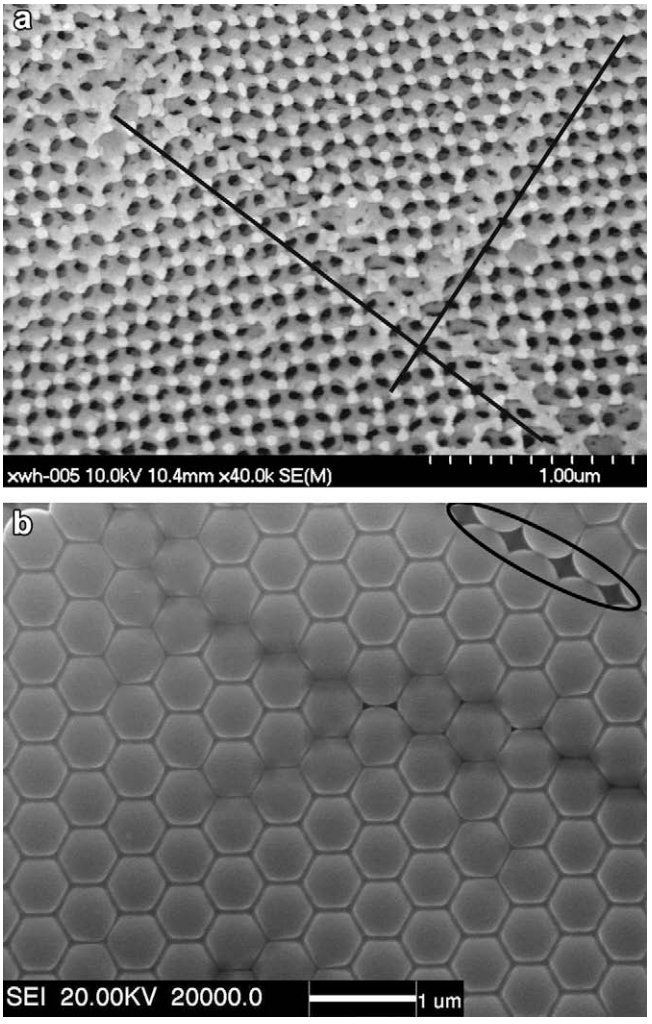

Fig. 4. SEM images showing (a) colloidal crystal with line defects and (b) the corresponding 3-DOM structure.

(marked with two lines). This kind of defects is mainly caused by the non-continuous capillary force during the self-assembly of PS templates.

The structures of the final 3-DOM Nb_2O_5 are strongly dependent on the precursor concentration. Fig. 5 shows SEM images of 3-DOM Nb_2O_5 prepared from Nb–citric precursor with different concentrations. At low concentration (0.2 mol/L), as shown in Fig. 5 (a), the wall of the 3-DOM Nb_2O_5 film is very thin and easy to be disrupted due to the low strength, which is resulted from the low solid content in the precursor after calcination. However, the wall structure of lower layers is of better condition because of the higher gravity of precursor to support the upside layers [22,23]. On the contrary, at high concentration (0.9 mol/L), as shown in Fig. 5(b), the high viscosity of the precursor will lead to a poor permeation and incomplete infiltration, the 3-DOM products collapse after calcination.

The cracks on the 3-DOM structure as shown in Fig. 6 (marked by arrows), which has been discussed by many researchers [24], are probably caused by the different expansion coefficients between the Nb_2O_5 products and the glass substrates during calcination.

The XPS measurement is employed to determine the surface composition of the 3-DOM Nb_2O_5. Fig. 7 shows the survey spectrum of product films, the signals of C, Si, O and Nb are visible. The existence of C1s peak is mainly caused by two factors: CO_2 adsorption or carbon compound from environment (contamination carbon). The core-level spectra of Nb in the Nb_2O_5 films are shown in the inset of Fig. 7. The Nb region exhibits the 3d5/2 and 3d3/2 transitions at 202.25 eV and 210.50 eV respectively [25,26]. The spectrum is characteristic of Nb_2O_5, indicating that the films are composed of Nb_2O_5.

FT-IR spectrum of the prepared Nb–citric precursor is shown in Fig. 8. The spectrum displays a strong peak at $\sim$3400 cm^{-1} which corresponds to the ν(OH) mode of (H-bonded) water molecules as well as the non-dissociated OH-group of the citric ligands. Pure citric acid has ν(C=O) mode at 1748 and 1715 cm^{-1}, but for the precursor the mode is absent. Instead, two intense peaks appear at 1641 and 1385 cm^{-1} which can be assigned to the $\nu_{as}(COO^-)$ and $\nu_s(COO^-)$ modes respectively [20]. And a characteristic peak at $\sim$700 cm^{-1} is generally assigned to the ν(Nb–O) mode, which indicates that the citric is chelate with Nb cations.

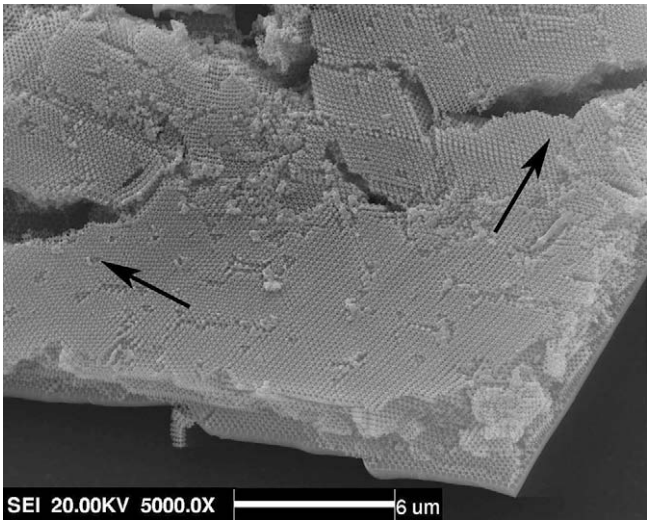

Fig. 6. SEM image showing the cracks on the 3-DOM structure.

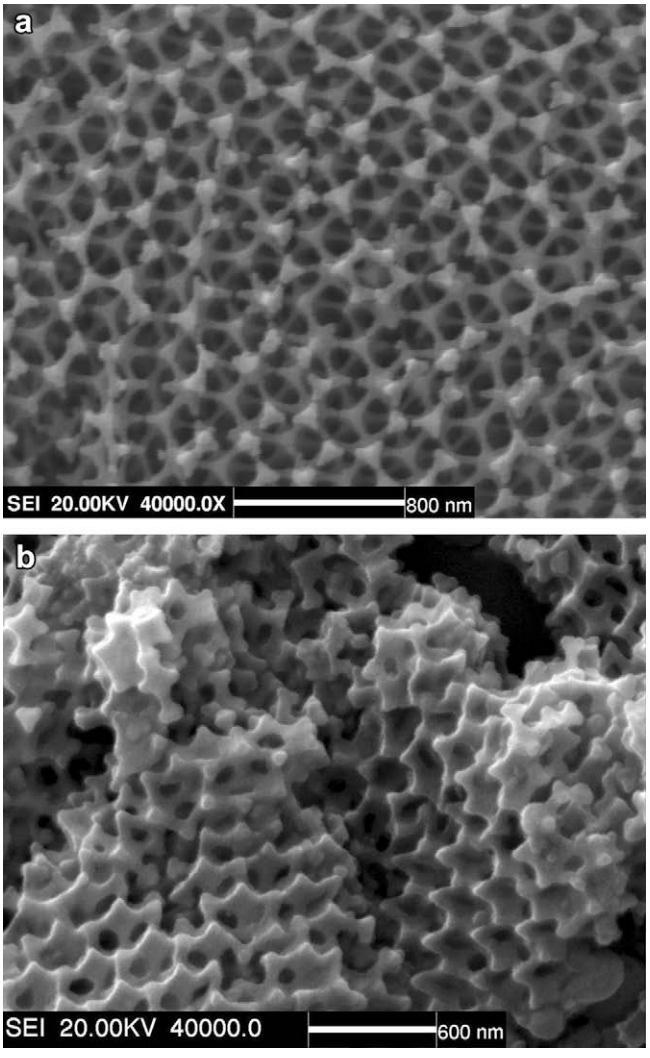

Fig. 5. SEM images showing the surfaces of 3-DOM Nb_2O_5 thin films infiltrated with Nb–citric precursors of different concentrations (a) 0.2 mol/L and (b) 0.9 mol/L.

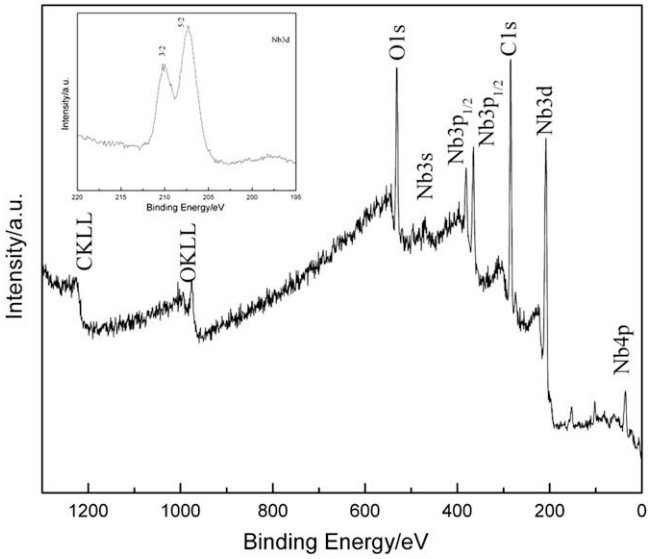

Fig. 7. Survey X-ray photoelectron spectrum of the 3-DOM Nb_2O_5 film. The inset is the higher resolution spectrum of Nb3d.

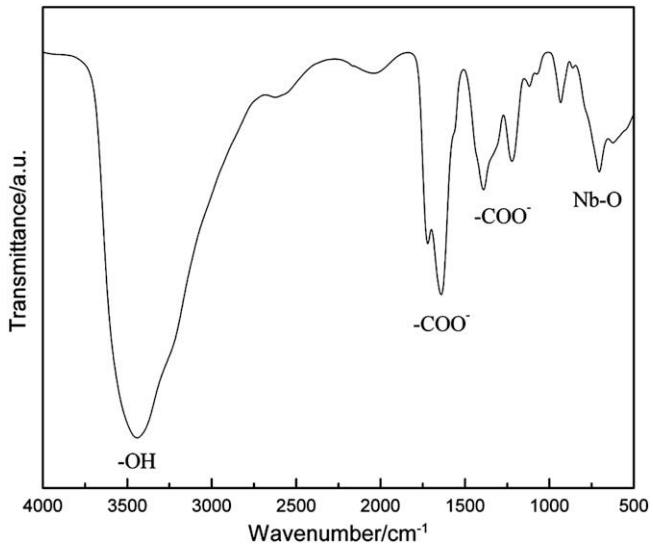

Fig. 8. FT-IR spectrum of niobium–citric sol.

Fig. 9 shows the X-ray diffraction (XRD) pattern of the macroporous samples calcined in air at 600 °C for 2 h. The peaks at $2\theta = 22.6°$ and 28.4° are respectively identified as the diffraction peaks of crystal faces (001) and (180) of monocline Nb_2O_5, indicating that the powder has a pure monocline phase [27].

The combined TG–DTA analysis (Fig. 10) was carried out to investigate the thermochemical behavior of the gel obtained from drying the Nb–citric precursor at 60 °C. The first weight loss region in the TG curve which accounted for ~30% of the total weight and occurred between 152 and 313 °C, is mainly due to evaporation of some residual water and desorption of molecular in the gel; the second weight loss region, which accounted for ~25% of the normalized weight, occurred between 313 and 462 °C, is associated with the oxidative decomposition of citric that was not chelate with Nb^{5+} ions; the last weight loss region occurred between 462 and 600 °C, accounted for ~18% of the sample's weight, is caused by the oxidative decomposition of the residual organics. The corresponding DTA curve reveals a single intense exothermic peak at 525 °C, indicating the oxidative decomposition [28]. The behavior

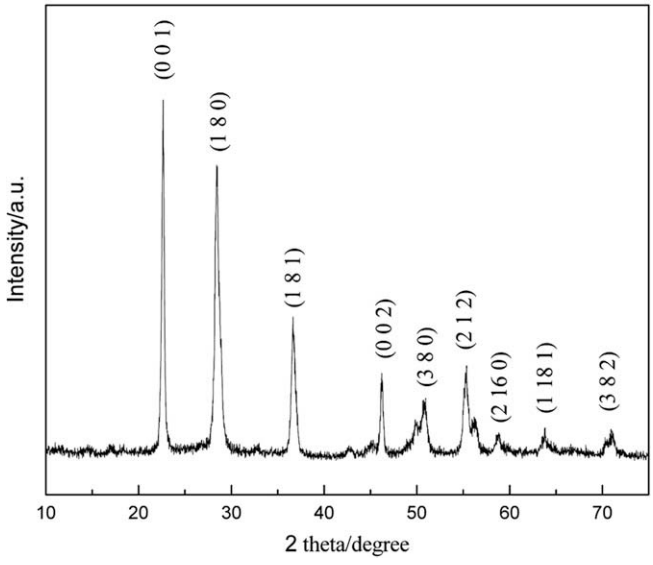

Fig. 9. X-ray diffractogram of 3-DOM Nb_2O_5 calcined in air at 600 °C for 2 h.

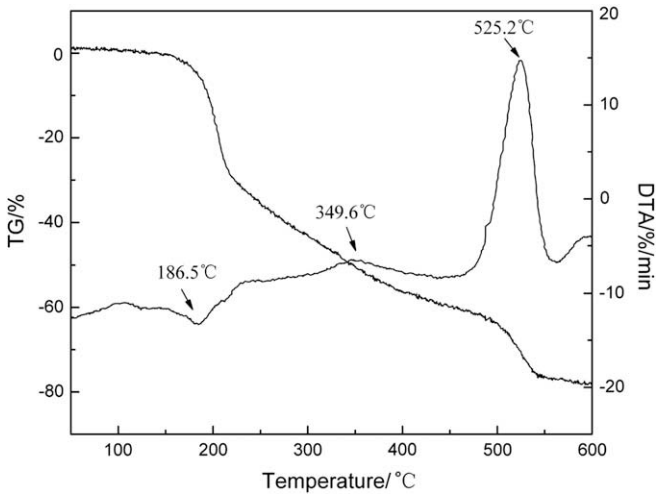

Fig. 10. TG/DTA curves of the gel obtained from drying the niobium–citric precursor at 60 °C.

of PS sphere has already been studied which indicates that all latex spheres were removed at a temperature of 450 °C [29]. Thus, the temperature of 600 °C used to complete the reaction to crystallize Nb_2O_5 is certainly sufficient to remove the template and obtain inverse opal.

4. Conclusions

Well-ordered macroporous niobium oxide materials were successfully prepared by using aqueous organic gel method with polystyrene templates. Stable Nb–citric complex was used as niobium precursor. The as-synthesized has both hexagonal and square packing arrays, influenced by different observation planes of PS templates. Point defects and line defects, the main two defects in colloidal crystal templates, are discussed in detail with the comparison between the colloidal templates and their negative replica. We demonstrate that the concentration of Nb–citric precursor had a great effect on the 3-DOM structure, the precursor with the concentration ranges from 0.2 to 0.8 mol/L can be used to fabricate 3-DOM structure. The results of XPS and FT-IR have confirmed that in the Nb–citric precursor, citric acid has coordinated to metal ions to form a complex. The desirable monocline phase has formed after calcination. The oxidation level of products is verified by XPS and the binding energies are in agreement with Nb_2O_5. The combined TG–DTA analysis was also carried out, and the curve illustrates that the temperature of 600 °C used to complete the reaction to crystallize Nb_2O_5 is certainly sufficient to remove the template and obtain inverse opal.

Acknowledgements

We thank the National Natural Science Foundation of China (No.20601006), CAST, the Program for New Century Excellent Talents in University and Natural Scientific Research Innovation Foundation in Harbin Institute of Technology (2008.04) for financial support.

References

[1] A. Imhof, D.J. Pine, Nature 389 (1997) 948.
[2] O.D. Vevel, T.A. Jede, R.F. Lobo, A.M. Lenhoff, Nature 389 (1997) 447.
[3] C.F. Blanford, H.W. Yan, R.C. Schroden, M. Al-Daous, A. Stein, Adv. Mater. 13 (2001) 401–407.
[4] B.T. Holland, C.F. Blanford, T. Do, A. Stein, Chem. Mater. 11 (1999) 795–805.
[5] H.Y. Shang, H. Mei, X.F. Zhou, Chin. J. Inorg. Chem. 24 (2008) 1812–1815.

[6] Z.L. Yang, H.Z. Chen, L. Cao, H.Y. Li, M. Wang, Mater. Lett. 58 (2004) 2238–2242.
[7] J. Choi, J.H. Lim, J. Lee, K.J. Kim, Nanotechnology 18 (2007) 055603.
[8] D.M. Antonelli, A. Nakahira, J.Y. Ying, Inorg. Chem. 35 (1996) 3126–3136.
[9] D.M. Antonelli, J.Y. Ying, Angew. Chem., Int. Ed. Engl. 35 (1996) 426–430.
[10] M.C. Orilall, N.M. Abrams, J. Lee, F.J. DiSalvo, U. Wiesner, J. Am. Chem. Soc. 130 (2008) 8882–8883.
[11] A. Blanco, E. Chomski, S. Grabtchak, M. Ibisate, S. John, S.W. Leonard, C. Lopez, F. Meseguer, H. Miguez, J.P. Mondia, G.A. Ozin, O. Toader, H.M. Direl, Nature 405 (2000) 437–438.
[12] O.D. Velev, P.M. Tessier, A.M. Lenho, E.W. Kaler, Nature 401 (1999) 548–550.
[13] J.E.G.J. Wijnhoven, S.J.M. Zevenhuizen, M.A. Hendriks, D. Vanmaekeibergh, J.J. Kelly, W.L. Vos, Adv. Mater. 12 (2000) 888–889.
[14] Y.G. Zhang, Z.B. Lei, J.M. Li, S.M. Lu, New J. Chem. 25 (2001) 1118–1120.
[15] Y. Li, J.P. Zhao, B. Wang, Mater. Res. Bull. 39 (2004) 365–374.
[16] R.N. Das, P. Pramanik, Mater. Lett. 46 (2000) 7–14.
[17] J.H. Kim, M. Chainey, M.S. El-Aasser, J.W. Vanderhoff, J. Polym. Sci., Part A: Polym. Chem. 27 (1989) 3187–3199.
[18] M.A. McLachlan, N.P. Johnson, R.M. RueLaDe, R.M. De La Rue, D.W. McComb, J. Mater. Chem. 14 (2004) 144–150.
[19] Y.Y. Zhou, Z.F. Qiu, M.K. Lü, A.Y. Zhang, Q. Ma, Mater. Res. Bull. 43 (2008) 1363–1368.
[20] J.P. Zhao, X.R. Liu, L.S. Qiang, Thin Solid Films 515 (2006) 1455–1460.
[21] N. Philip, T.D. Bartlett, A.G. Mohamed, J. Mater. Chem. 12 (2002) 3130–3135.
[22] Y.N. Fu, Z.G. Jin, Z.F. Liu, W. Li, J. Eur. Ceram. Soc. 27 (2007) 2223–2228.
[23] J.P. Zhao, Y. Li, W.H. Xin, X. Li, J. Solid State Chem. 181 (2008) 239–244.
[24] M.A. McLachlan, N.P. Johnson, R.M. De La Rue, D.W. McComb, J. Mater. Chem. 14 (2004) 144–150.
[25] M. Selvaraj, S. Kawi, D.W. Park, C.S. Ha, J. Phys. Chem. C 113 (2009) 7743–7749.
[26] E. Ramirez-Cabrera, A. Atkinson, D. Chadwick, Appl. Catal., B: Environ. 36 (2002) 193–206.
[27] R. Kodama, Y. Terada, I. Nakai, S. Komaba, N. Kumagai, J. Electrochem. Soc. 153 (2006) A583–A588.
[28] N. Petrova, D. Todorovsky, Mater. Res. Bull. 41 (2006) 576–589.
[29] Y. Jin, Y.H. Zhu, X.L. Yang, C.Z. Li, J.H. Zhou, J. Solid State Chem. 180 (2007) 300–305.